Optická emisní spektroskopie atomů

Diagnostické metody 1

Zdeněk Navrátil

Ústav fyzikální elektroniky Přírodovědecké fakulty Masarykovy univerzity, Brno

Outline

1. OES
2. CR modelling
3. CR model for neon discharge
4. Examples
    - DC
    - RF
    - MW
5. Measurement of densities by self-absorption methods

Instrumentation

- typically grating spectrometer of Czerny-Turner mounting equipped with CCD/ICCD detector
- typical spectral range 190 – 1100 nm
- sensitivity of detectors (silicon CCD, photocathode of PMT), grating efficiency
- resolution: number of illuminated grating grooves, slit width, pixel size

$$R = \lambda/\Delta\lambda = mN$$

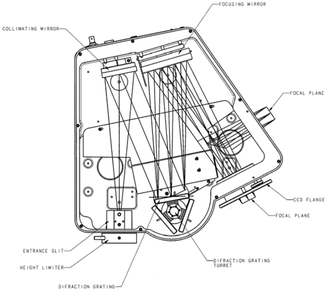

Sensitivities

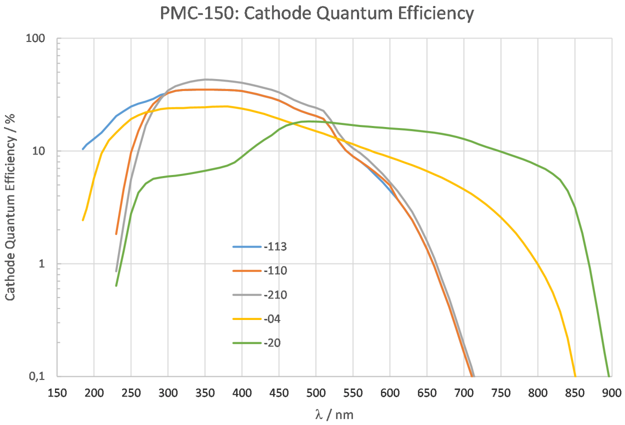

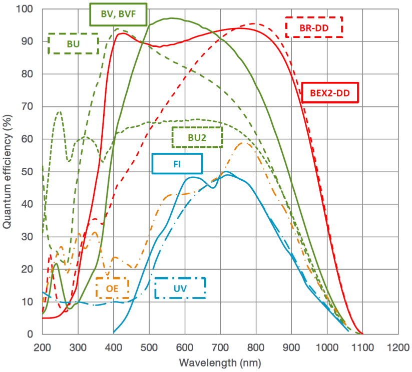

- grating efficacy, fibre efficacy, windows

Technique overview – how we measure

- collecting the light emitted by plasma (optical emission spectroscopy, OES):
  - non-intrusive
  - sensing the light at the plasma boundary
  - optical probes
- sending the light through the plasma (optical absorption spectroscopy):
  - based on Lambert-Beer law
  - can disturb the plasma, two ports
  - white light, hollow cathode lamps, lasers
- collecting the light emitted and reabsorbed by the plasma (self-absorption methods of OES)

Technique overview – how we measure

- collecting the light emitted by plasma (optical emission spectroscopy, OES):
  - non-intrusive
  - sensing the light at the plasma boundary $\rightarrow$ self-absorption can play a role
  - optical probes
- sending the light through the plasma (optical absorption spectroscopy):
  - based on Lambert-Beer law
  - can disturb the plasma, two ports
  - white light, hollow cathode lamps, lasers
- collecting the light emitted and reabsorbed by the plasma (self-absorption methods of OES)

Technique overview – what we look at

- line positions = wavelengths: electric, magnetic fields, atom velocities (Stark, Zeeman, Doppler effect)
- lineshapes and linewidths: electron density, gas pressure, density, temperatures (Stark, van der Waals, resonance, Doppler line broadening)
- line intensities: . . . all

Technique overview – what we look at

- line positions = wavelengths: electric, magnetic fields, atom velocities (Stark, Zeeman, Doppler effect)
- lineshapes and linewidths: electron density, gas pressure, density, temperatures (Stark, van der Waals, resonance, Doppler line broadening)
- line intensities: . . . all
  - relative – instrument spectral sensitivity is taken into account, no absolute intensity calibration is performed
    output: relative populations of excited states, excitation temperatures etc.
  - absolute – access to absolute densities of excited states, electron density etc.

Absolute intensity measurement

- radiant flux/zářivý tok – energy emitted/incident on surface per unit time

$$\Phi = \frac{\mathrm{d}\mathscr{E}}{\mathrm{d}t}, \quad \mathrm{W} \tag{1}$$

- irradiance – flux density (per unit surface)

$$I = \frac{\mathrm{d}\Phi}{\mathrm{d}S} = \frac{\mathrm{d}^2\mathscr{E}}{\mathrm{d}t\mathrm{d}S}, \quad \mathrm{W\,m^{-2}} \tag{2}$$

  - specified during calibratrion of calibrated light sources (spectral irradiance)
  - optical fibre is not a detector of irradiance (acceptance angle)
  - radiometric irradiance probes, cosine correction diffusers, integrating spheres, . . .

Absolute intensity measurement 2

- radiance (zář) – radiant flux per unit perpendicular surface and unit solid angle

$$L = \frac{\mathrm{d}^2\Phi}{\mathrm{d}S\cos\theta\,\mathrm{d}\Omega} = \frac{\mathrm{d}^3\mathscr{E}}{\mathrm{d}t\,\mathrm{d}S\cos\theta\,\mathrm{d}\Omega}, \quad \mathrm{W\,m^{-2}\,sr^{-1}} \tag{3}$$

- radiance × irradiance

$$I = \int_{\Omega} L(\theta)\cos\theta\,\mathrm{d}\Omega \tag{4}$$

For constant L (Lambert) radiators $I = \pi L$.

- for description of radiating solid surfaces

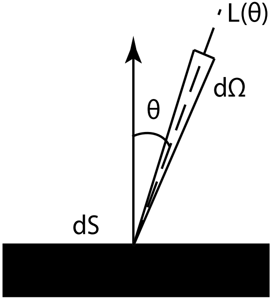

Absolute intensity measurement 3

- emission coefficient – radiant power emited by unit volume into unit solid angle

$$j = \frac{\mathrm{d}^3\mathscr{E}}{\mathrm{d}t\,\mathrm{d}V\,\mathrm{d}\Omega}. \quad (5)$$

- all quantities have their spectral densities, e.g. $j(\lambda)$

emission coefficient of transition

$$j_{ij} = \frac{1}{4\pi} n_i A_{ij} h\nu_{ij}$$

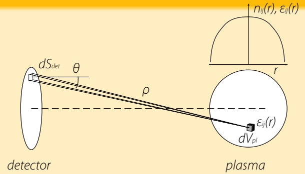

$$I_{ij} = \frac{1}{S_{\mathrm{det}}} \int_{V_{\mathrm{pl}}} \int_{S_{\mathrm{det}}} \frac{j_{ij}(r)}{\rho^2} \mathrm{Acc}(\theta) \mathrm{d}V_{\mathrm{pl}} \mathrm{d}S_{\mathrm{det}}$$

irradation of detector for optical thin plasma condition

Electron temperature from Boltzmann plot?

- density of atoms in excited state

$$n_i = n \frac{g_i}{Q} \mathrm{e}^{-\frac{\mathscr{E}_i}{k_\mathrm{b} T_\mathrm{e}}} \tag{6}$$

2 g_i – statistical weight, $\mathscr{E}_i$ – excitation energy, n – atom density, Q – state sum, T_e excitation ($\stackrel{?}{=}$ electron) temperature

- spectral line intensity

$$I \propto n_i A_{ij} \frac{hc}{\lambda} \tag{7}$$

$$I = C \cdot \frac{g_i A_{ij}}{\lambda} \mathrm{e}^{-\frac{\mathscr{E}_i}{k_\mathrm{b} T_\mathrm{e}}} \tag{8}$$

- Boltzmann plot

$$\ln \frac{I\lambda}{g_i A_{ij}} = -\frac{1}{k_\mathrm{b} T_\mathrm{e}} \mathscr{E}_i + \ln k_1, \tag{9}$$

Possibility of electron temperature measurement

excited level balance

- local thermodynamic equilibrium (LTE) plasma
  - LTE condition

$$n_e \gg 1.6 \cdot 10^{12} \sqrt{T_e} (\Delta E)^3 \quad (\mathrm{cm}^{-3})$$

  - electron temperature from Boltzmann plot
- non-LTE plasma
  - corona equilibrium, excitation saturation phase, . . .
  - low electron density plasma
  - use of Boltzmann-plot leads to erroneous electron temperature
  - CR modelling

non-Maxwellian EDF

- inelastic collisions, beam electrons, non-local EDF

Collisional-radiative modelling

coupled DE for densities of excited states

$$\frac{\partial n_i}{\partial t} + \nabla(n_i\vec{v}) = \left(\frac{\partial n_i}{\partial t}\right)_{\mathrm{c,r}} \quad (10)$$

population and depopulation processes are very fast:

$$\frac{\partial n_i}{\partial t} = \left(\frac{\partial n_i}{\partial t}\right)_{\mathrm{c,r}} = 0 \quad (11)$$

not valid for ground-state atoms, ions, metastables, high pressure

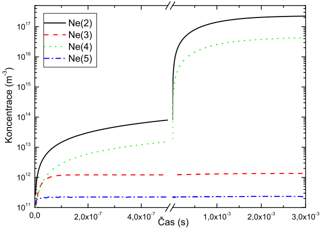

Level balance

$$\frac{\partial n_0}{\partial t} + \nabla(n_0 \vec{v_0}) = -S_{\rm cr} n_{\rm e} n_0 + \alpha_{\rm cr} n_{\rm e} n_{\rm ion}$$

$$\frac{\partial n_{\rm ion}}{\partial t} + \nabla(n_{\rm ion} \vec{v_{\rm ion}}) = +S_{\rm cr} n_{\rm e} n_0 - \alpha_{\rm cr} n_{\rm e} n_{\rm ion}$$

classification of models (plasma state)

- ionizing plasma $S_{\rm cr} n_{\rm e} n_0 - \alpha_{\rm cr} n_{\rm e} n_{\rm ion} > 0$
  - plasma conducting current, ionizing waves
- recombining plasma $S_{\rm cr} n_{\rm e} n_0 - \alpha_{\rm cr} n_{\rm e} n_{\rm ion} < 0$
  - afterglows, outer regions of flames
- equilibrium plasma $S_{\rm cr} n_{\rm e} n_0 - \alpha_{\rm cr} n_{\rm e} n_{\rm ion} = 0$ (ioniozation-recombination equilibrium)

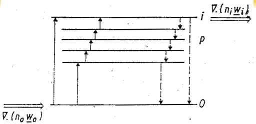

ionizing plasma

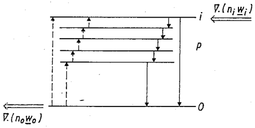

recombining plasma

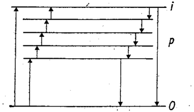

equilibrium plasma

Excitation phases: corona phase

population by electron impact excitation, radiative deexcitation

$$k_{0i}^{\mathrm{el}} n_{\mathrm{e}} n_0 + k_{\mathrm{m}i}^{\mathrm{el}} n_{\mathrm{e}} n_{\mathrm{m}} \left(+ \sum_{j>i} \Lambda_{ji} A_{ji} n_j\right) = \sum_{j<i} \Lambda_{ij} A_{ij} n_i \tag{12}$$

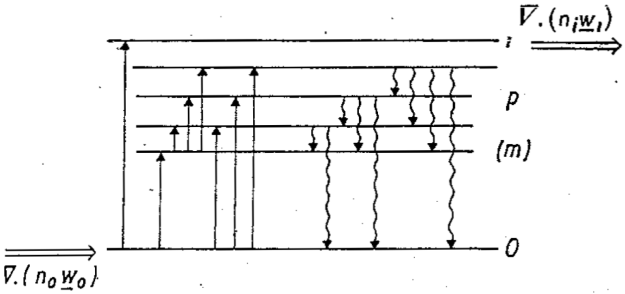

Excitation phases: excitation saturation phase

population and depopulation by electron impact

$$\sum_{j \neq i} k_{ji}^{\mathrm{el}} n_{\mathrm{e}} n_j + (\alpha_i n_{\mathrm{e}} n_{\mathrm{ion}}) = \sum_{j \neq i} k_{ij}^{\mathrm{el}} n_{\mathrm{e}} n_i + S_i n_{\mathrm{e}} n_i$$

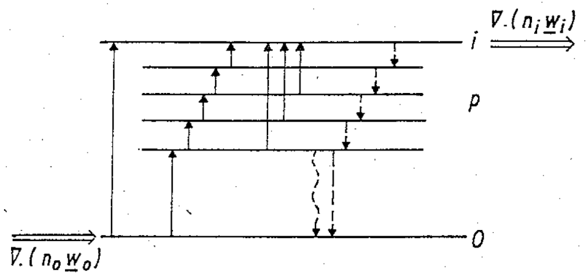

- saturation of the excited state densities with increased n_{e}
- no Saha equilibrium, $S_i n_i \gg \alpha_i n_{\mathrm{ion}}$

Excitation phases: excitation saturation phase 2

- stepwise excitation → ladder-like excitation flow
- coefficients of upward processes are larger (closer upper levels, higher statistical weights of upper levels)

$$k_{i-1,i} n_{\mathrm{e}} n_{i-1} - k_{i,i-1} n_{\mathrm{e}} n_i = k_{i,i+1} n_{\mathrm{e}} n_i - k_{i+1,i} n_{\mathrm{e}} n_{i+1} - S_i n_{\mathrm{e}} n_i$$

Excitation phases: partial local thermodynamic equilibrium

- 2 equilibria: excited state × ion state, neighbouring excited states
- ionization ∼ recombination ≫ excitation flow

$$k_{i-1,i} n_e n_{i-1} - k_{i,i-1} n_e n_i = k_{i,i+1} n_e n_i - k_{i+1,i} n_e n_{i+1} - S_i n_e n_i + \alpha_i n_e n_{ion}$$

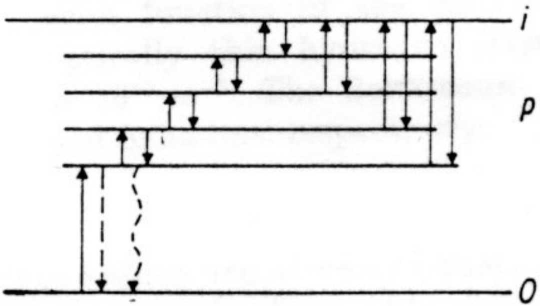

Role of dominant electron collisions

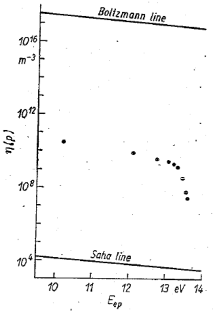

$n_e = 10^{16}$ m^{-3}

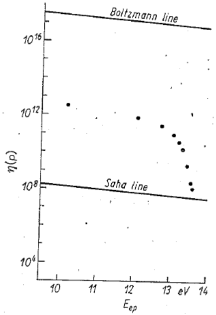

$n_e = 10^{18}$ m^{-3}

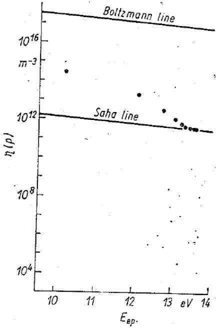

$n_e = 10^{20}$ m^{-3}

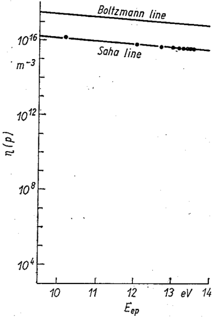

$n_e = 10^{22}$ m^{-3}

Boltzmann	$n_i^B = n_0 g_i / g_0 \mathrm{e}^{-E_i/kT_\mathrm{e}}$
Saha	$n_i^S = n_\mathrm{e} n_\mathrm{ion} \frac{g_i}{g_e g_\mathrm{ion}} (h^2/2\pi m_\mathrm{e} k T_\mathrm{e})^{3/2} \mathrm{e}^{E_{ion,i}/kT_\mathrm{e}}$
deviation from B & S	$n_i = r_i^0 n_i^S + r_i^1 n_i^B$

Excitation phases

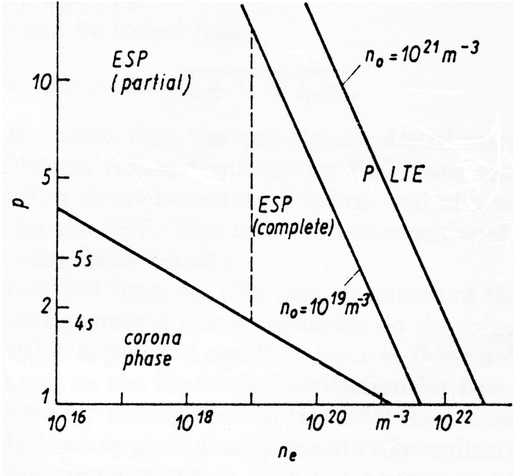

Collisional-radiative model

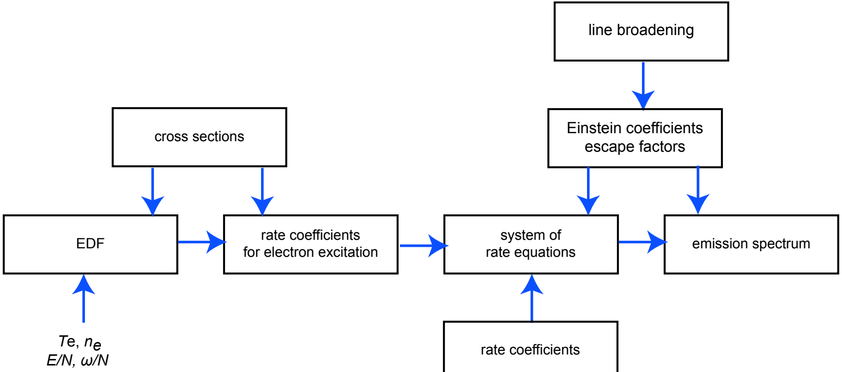

Electron distribution function

- Maxwellian EDF
- solution of Boltzmann kinetic equation
- normalization of the EDF

$$\int_0^\infty f(\varepsilon)\varepsilon^{1/2}\mathrm{d}\varepsilon = 1 \tag{13}$$

- mean electron energy

$$\langle\varepsilon\rangle = \int_0^\infty f(\varepsilon)\varepsilon^{3/2}\mathrm{d}\varepsilon, \tag{14}$$

- rate coefficients k, k_{inv} of electron collision with cross section σ and of inverse process

$$k = \sqrt{\frac{2e}{m_\mathrm{e}}}\int_0^\infty \sigma(\varepsilon)f_0(\varepsilon)\varepsilon\mathrm{d}\varepsilon$$

$$k_{\mathrm{inv}} = \sqrt{\frac{2e}{m_\mathrm{e}}\frac{g_j}{g_i}}\int_{\varepsilon_{ij}}^\infty \sigma(\varepsilon)f_0(\varepsilon-\varepsilon_{ij})\varepsilon\mathrm{d}\varepsilon$$

Approaches of OES data processing

- line ratio methods
  - selection of convenient line pair (sensitivity, model simplicity, ease of measurement)
  - no control of model validity
- „many line fitting“methods

Line ratio method – ideal case

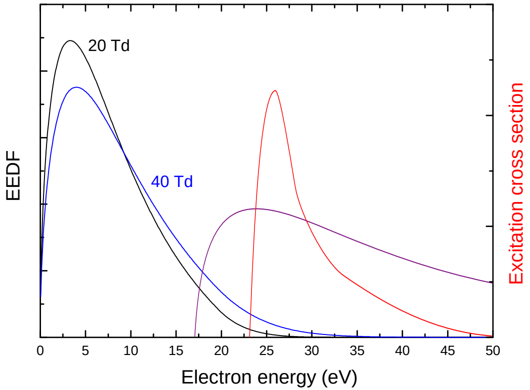

Electron temperature and EDF measurement by OES+CR

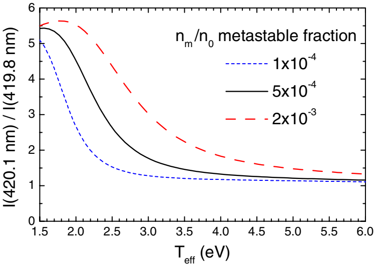

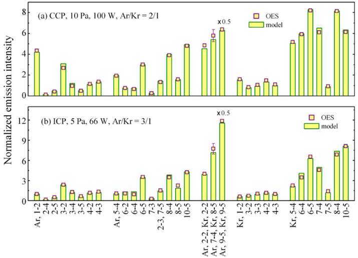

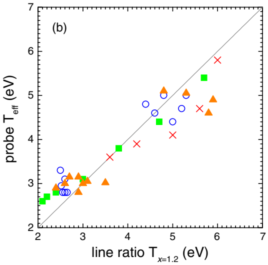

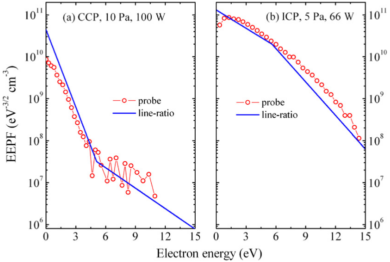

Electric field measurement in air

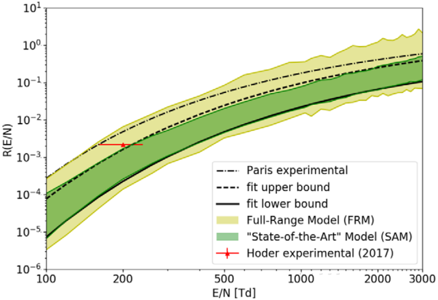

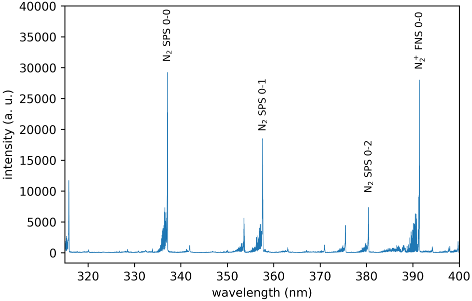

$$R(E/N) = \frac{FNS(0,0)}{SPS(0,0)}$$

Kozlov and Wagner 2001 *J. Phys. D: Appl. Phys.* **34** 3164
Bilek *et al* 2018 *Plasma Sources Sci. Technol.* **27** 085012

TRG spectroscopy

- based on admixing of a small amount of rare gas into plasma
- mapping EDF at specific electron energies
- low pressure, what is small amount?

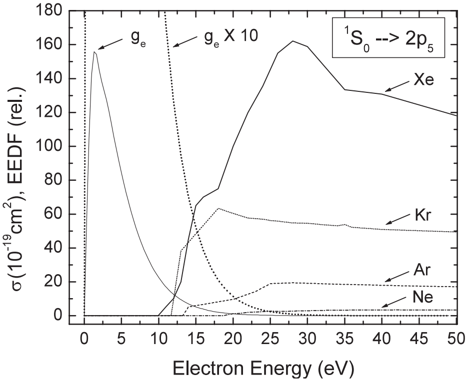

Helium line ratio method

- ratio of helium singlet lines $R = I_{667}/I_{728}$
  He I 667.8 nm ($2\ ^1P - 3\ ^1D$)
  He I 728.1 nm ($2\ ^1P - 3\ ^1S$)

✓ high spectral resolution is not required

✓ sensitive to fields of several kV/cm

✓ verified at atmospheric pressure

✗ dependence on the gas purity

✗ dependence on metastable density at low field

$$E(R) = 2.224 - 20.18R + 45.07R^2 - 19.98R^3 + 3.369R^4$$
$[E] =$ kV/cm, for 3−40 kV/cm, $T = 310$ K

Ivković et al 2014 *J. Phys. D: Appl. Phys.* **47** 055204

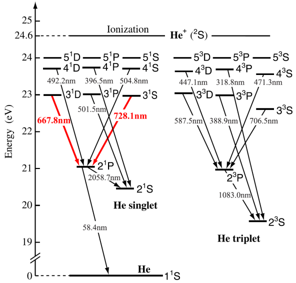

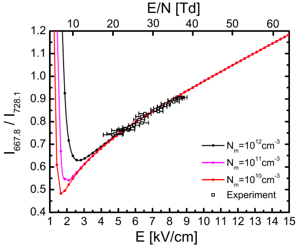

Diffuse coplanar barrier discharge in rare gases

Neon

diffuse,
high gas purity

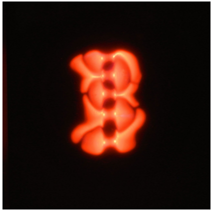

filamentary,
low gas purity

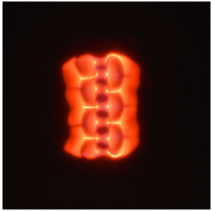

low gas purity,
higher voltage

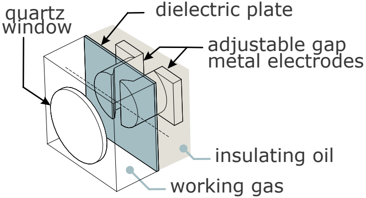

Helium

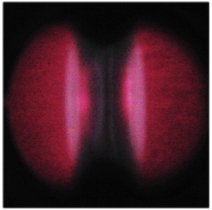

50 ms

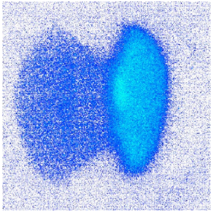

1 µs

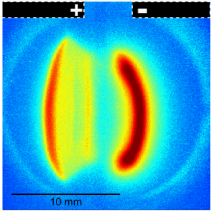

100 ns, 10 k

run:I.mp4

Experimental setup

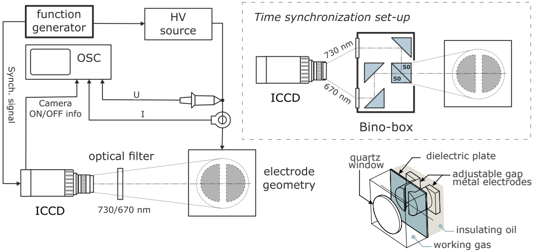

- coplanar DBD, brass electrodes covered with 96% Al_2O_3 (0.63 mm thick),
- parallel gap footprint, electrode distance 4.75 mm,
- helium 5.0 at atmospheric pressure, gas flow 550 sccm
- AC sine-wave high voltage of 1.6 kVmax, 10.3 kHz
- ICCD camera Princeton Instruments PI-MAX3 (time window 50 ns)
- bandpass filters Thorlabs FL670-10 and FL730-10 (670, 730 nm, FWHM 10 nm)

2D resolved electric field development

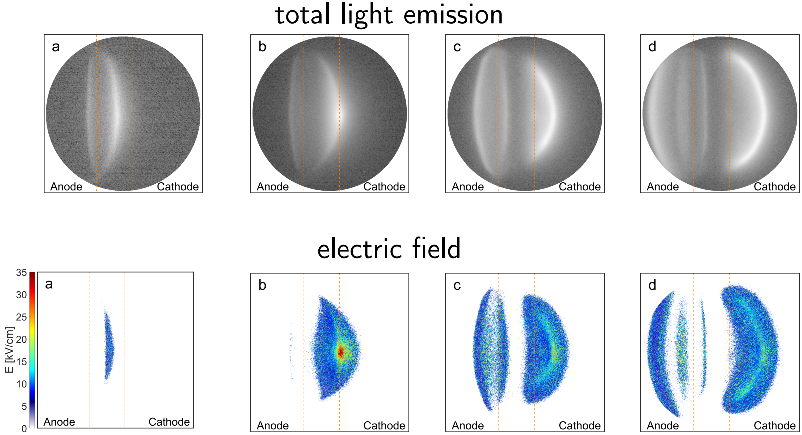

CDIW: $\sim$ 10 kV/cm $\sim$ 32 kV/cm 20 – 25 kV/cm

Čech J *et al* 2D-resolved electric field development in helium coplanar DBD *Plasma Sources Sci. Technol.* **27** 105002

2D resolved simultaneous line ratio measurement

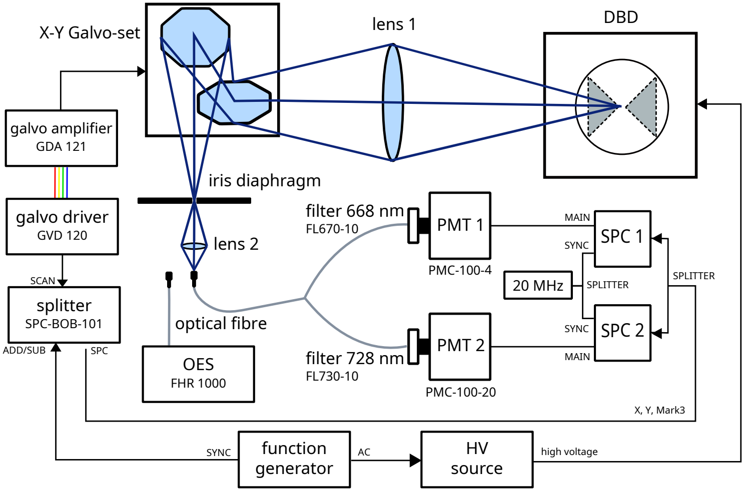

Excited levels

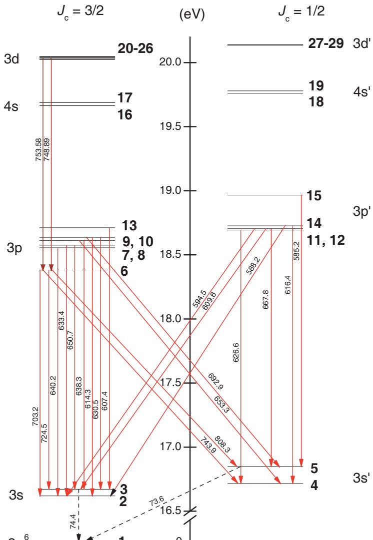

i	nlpqr	Racah	Paschen		(eV)
1	21000	$2p^6$	$1p_0$	1	0.000000
2	30332	$3s\ [3/2]^o_2$	$1s_5$	5	16.61907
3	30331	$3s\ [3/2]^o_1$	$1s_4$	3	16.67083
4	30110	$3s'\ [1/2]^o_0$	$1s_3$	1	16.71538
5	30111	$3s'\ [1/2]^o_1$	$1s_2$	3	16.84805
6	31311	$3p\ [1/2]_1$	$2p_{10}$	3	18.38162
7	31353	$3p\ [5/2]_3$	$2p_9$	7	18.55511
8	31352	$3p\ [5/2]_2$	$2p_8$	5	18.57584
9	31331	$3p\ [3/2]_1$	$2p_7$	3	18.61271
10	31332	$3p\ [3/2]_2$	$2p_6$	5	18.63679
11	31131	$3p'\ [3/2]_1$	$2p_5$	3	18.69336
12	31132	$3p'\ [3/2]_2$	$2p_4$	5	18.70407
13	31310	$3p\ [1/2]_0$	$2p_3$	1	18.71138
14	31111	$3p'\ [1/2]_1$	$2p_2$	3	18.72638
15	31110	$3p'\ [1/2]_0$	$2p_1$	1	18.96596
16	40332	$4s\ [3/2]^o_2$	$2s_5$	5	19.66403
17	40331	$4s\ [3/2]^o_1$	$2s_4$	3	19.68820
18	40110	$4s'\ [1/2]^o_0$	$2s_3$	1	19.76060
19	40111	$4s'\ [1/2]^o_1$	$2s_2$	3	19.77977
20	32310	$3d\ [1/2]^o_0$	$3d_6$	1	20.02464
21	32311	$3d\ [1/2]^o_1$	$3d_5$	5	20.02645
22	32374	$3d\ [7/2]^o_4$	$3d'_4$	9	20.03465
23	32373	$3d\ [7/2]^o_3$	$3d_4$	7	20.03487
24	32332	$3d\ [3/2]^o_2$	$3d_3$	5	20.03675
25	32331	$3d\ [3/2]^o_1$	$3d_2$	3	20.04039
26	32352	$3d\ [5/2]^o_2$	$3d''_1$	5	20.04821
	32353	$3d\ [5/2]^o_3$	$3d'_1$	7	20.04843
27	32152	$3d'\ [5/2]^o_2$	$3s''''_1$	5	20.13611
	32153	$3d'\ [5/2]^o_3$	$3s'''_1$	7	20.13630
28	32132	$3d'\ [3/2]^o_2$	$3s''_1$	5	20.13751

Considered elementary processes

1. Electron impact excitation out of the g.s.

$$\mathrm{Ne}(1)+\mathrm{e}^- \xrightarrow{k_{1j}} \mathrm{Ne}(j)+\mathrm{e}^-, \quad j=2,\dots 29$$

2. Electron impact excitation out of $2p^5 3s$ states

$$\mathrm{Ne}(i)+\mathrm{e}^- \xrightarrow{k_{ij}} \mathrm{Ne}(j)+\mathrm{e}^-, \quad i=2,\dots 5,\ j=6,\dots 15$$

3. Electron impact deexcitation to the g.s. and $2p^5 3s$ states

$$\mathrm{Ne}(i)+\mathrm{e}^- \xrightarrow{k_{ij}} \mathrm{Ne}(j)+\mathrm{e}^-, \quad i=2,\dots 29,\ j=1,\dots 5,\ i>j$$

4. Electron induced excitation transfer among $2p^5 3s$ states

$$\mathrm{Ne}(i)+\mathrm{e}^- \xrightarrow{k_{ij}} \mathrm{Ne}(j)+\mathrm{e}^-, \quad i,j=2,\dots 5$$

5. Spontaneous emission and absorption of radiation

$$\mathrm{Ne}(i) \xrightarrow{\Lambda_{ij}A_{ij}} \mathrm{Ne}(j)+h\nu, \quad i=2,\dots 29,\ i>j$$

Considered elementary processes 2

6. Two-body collision induced deactivation and excitation transfer among $2p^5 3p$ states

$$\mathrm{Ne}(i) + \mathrm{Ne}(1) \xrightarrow{k_{ij}} \mathrm{Ne}(j) + \mathrm{Ne}(1), \quad i,j = 6,\ldots 15$$

7. Chemoionization

$$\mathrm{Ne}(2-5) + \mathrm{Ne}(2-5) \xrightarrow{k_{\mathrm{met}}} \mathrm{Ne}(1) + \mathrm{Ne}^+ + \mathrm{e}^-$$

8. Two-body collision induced deactivation

$$\mathrm{Ne}(2-5) + \mathrm{Ne}(1) \xrightarrow{k_{2\mathrm{b}}} 2\mathrm{Ne}(1)$$

9. Penning ionization of impurities

$$\mathrm{Ne}(2\text{-}5) + \mathrm{H}_2 \xrightarrow{k_{\mathrm{H_2}^+}} \mathrm{H_2}^+ + \mathrm{Ne}(1) + \mathrm{e}^-$$

$$\mathrm{Ne}(2\text{-}5) + \mathrm{H}_2 \xrightarrow{k_{\mathrm{NeH}^+}} \mathrm{NeH}^+ + \mathrm{H} + \mathrm{e}^-$$

$$\mathrm{Ne}(2\text{-}5) + \mathrm{N}_2 \xrightarrow{k_{\mathrm{N_2}^+}} \mathrm{N_2}^+ + \mathrm{Ne}(1) + \mathrm{e}^-$$

Considered elementary processes 3

12. Electron impact ionization of the ground-state and metastable atoms
13. Three-body production of dimers

$$\mathrm{Ne}(2,4) + \mathrm{Ne}(1) + \mathrm{Ne}(1) \xrightarrow{k_{3\mathrm{bm}}} \mathrm{Ne}_2^* + \mathrm{Ne}(1)$$

$$\mathrm{Ne}(3) + \mathrm{Ne}(1) + \mathrm{Ne}(1) \xrightarrow{k_{3\mathrm{b}_3}} \mathrm{Ne}_2^{\mathrm{m}} + \mathrm{Ne}(1)$$

$$\mathrm{Ne}(5) + \mathrm{Ne}(1) + \mathrm{Ne}(1) \xrightarrow{k_{3\mathrm{b}_5}} \mathrm{Ne}_2^{\mathrm{m}} + \mathrm{Ne}(1)$$

Spontaneous emission

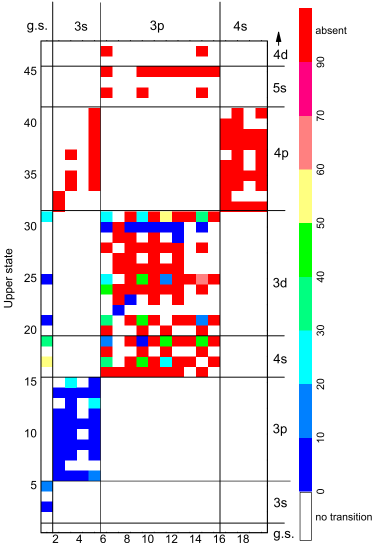

Einstein coefficient A_{ij}

$$A_{ij} = \frac{16\pi^3 \nu^3}{3\varepsilon_0 hc^3} \frac{S}{g_i}$$

$$A_{ij} = \frac{g_j}{g_i} \frac{2\pi e^2 \nu^2}{\varepsilon_0 mc^3} f$$

effective levels

$$A_{\{i\}j} = \frac{\sum_i g_i A_{ij}}{\sum_i g_i}$$

← relative differences of two data source – NIST and Seaton 1998

Absorption of radiation

Number of absorption transitions between states i, j (j is lower) in unit volume is

$$n_j B_{ji} \rho(\omega_0)$$

What is $\rho(\omega_0)$?

The spatial distribution of population of excited state due to the radiation propagation can be described by Holstein equation

$$\frac{\partial n(\vec{r})}{\partial t} = -An(\vec{r}) + A \int n(\vec{r}')G(\vec{r}',\vec{r})\mathrm{d}\vec{r}', \quad (15)$$

$$G(\vec{r}',\vec{r}) = -\frac{1}{4\pi\rho^2}\frac{\partial T}{\partial \rho}, \rho = |\vec{r}' - \vec{r}|, \quad T(\rho) = \int f(\omega)\mathrm{e}^{-kf(\omega)\rho}\mathrm{d}\omega.$$

Solution of Holstein equation has a form

$$n(\vec{r},t) = \sum_j c_j n_j(\vec{r})\mathrm{e}^{-A/g_j t}, \quad (16)$$

in which g_j are *trapping* factors attached to eigenfunctions n_j. Escape factor $\Lambda = 1/g_0$.

Trapping factor

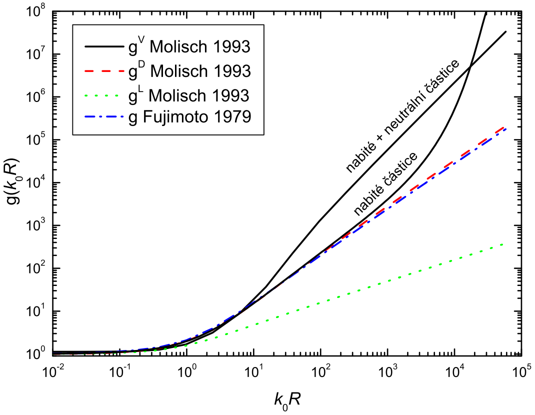

Parameters of solution:

- discharge geometry
- opacity $k_0 R$
- spectral line profile

Solution of rate-equations

Initial conditions

$$n_i(t=0) = \begin{cases} N \equiv \frac{p}{k_\mathrm{b} T_\mathrm{n}}, & i = 1 \\ 0, & i > 1 \end{cases} \quad (17)$$

- Runge-Kutta methods
- stationary state solution: all excited states reach stationary state ($\frac{\partial n_i}{\partial t} = 0$)
- Non-linear dependence of some rate equations

$$\left(\frac{\partial n_2}{\partial t}\right)_\mathrm{met} = -4k_\mathrm{met} n_2^2 - 2k_\mathrm{met} n_2 n_4 - \ldots - (k_{\mathrm{H_2^+}} + k_{\mathrm{NeH^+}})[\mathrm{H_2}] n_2 - -(k_{\mathrm{N_2^+}} + k_{\mathrm{NeN_2^+}})[\mathrm{N_2}] n_2 - k_{\mathrm{O_2^+}}[\mathrm{O_2}] n_2 - \frac{D_2}{l_\mathrm{D}^2} n_2 - k_\mathrm{ionmet} n_\mathrm{e} n_2$$

Spectrum calculation and comparison

- measured spectral line intensities, integrated over lineshapes

$$[\lambda_k, I_k^{\mathrm{exp}}],\ k = 1, \dots n,\ n = 30$$

- calculated total emission coefficients of transitions

$$I_{ij}^{\mathrm{cr}} = \frac{1}{4\pi} n_i \Lambda_{ij} A_{ij} h\nu_{ij}$$

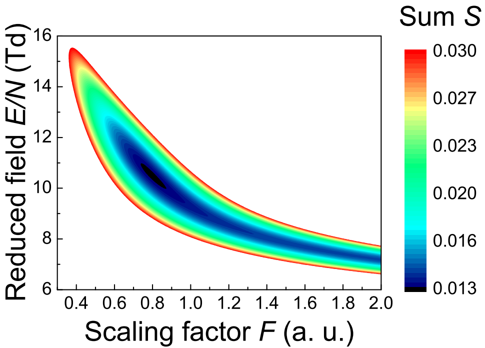

- comparison of spectra by least squares method

$$\mathscr{S} = \sum_{k=1}^{n} \frac{(\mathscr{F} \cdot I_k^{\mathrm{cr}}(T_e, n_e, n_{1s_3}, n_{1s_5}) - I_k^{\mathrm{exp}})^2}{I_k^{\mathrm{exp}}}$$

Role of metastables

- simplified 0D scheme is not valid

$$\frac{\partial n_i}{\partial t} + \nabla(n_i \vec{v}) = \left(\frac{\partial n_i}{\partial t}\right)_{\mathrm{c,r}} \qquad (18)$$

- longer computational times
- increased sensitivity at low electron energies

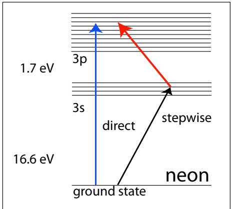

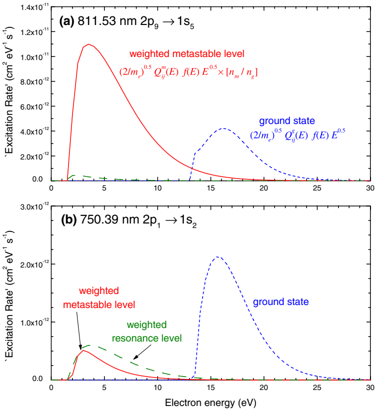

argon

Boffard J B, Jung R O, Lin C C and Wendt A E 2010

Direct and stepwise excitation

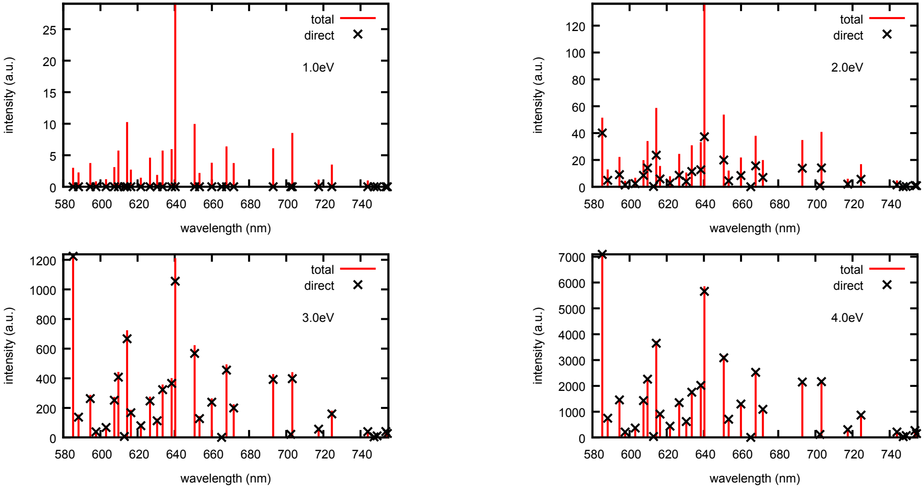

Maxwellian EDF, gas temperature 300 K, fixed densities of all $1s_i$ levels

DC glow discharge in neon

- positive column of DC glow discharge at 1.1 Torr
- OES in spectral range 300 – 850 nm
- CR model with stationary BKE solver
- probe measurement

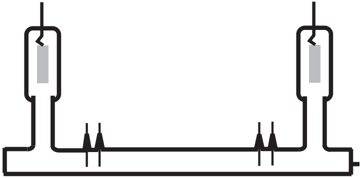

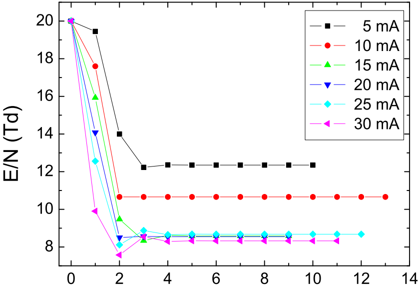

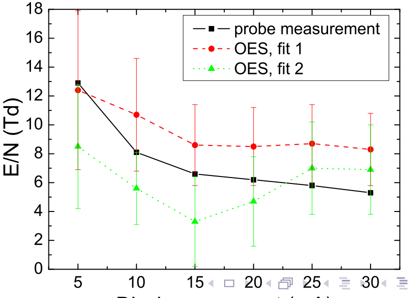

Radio-frequency discharge in neon

- capacitively coupled RF discharge in neon (13.56 MHz)
- low pressure (10 Pa)
- reactor R3 "Temelín", inner diameter 33 cm, discharge gap 40 mm, electrodes 8 cm in diameter
- studied by OES/CR, OAS, PIC/MC, Langmuir probe
- absolute intensity measurement

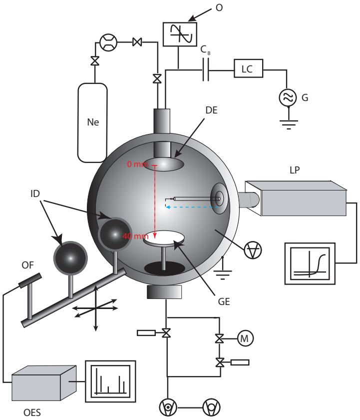

RF (13.56 MHz) capacitive discharge in neon at 10 Pa

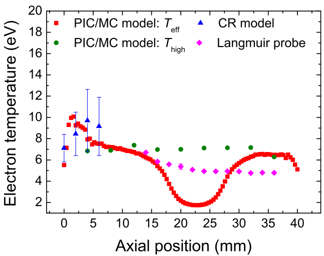

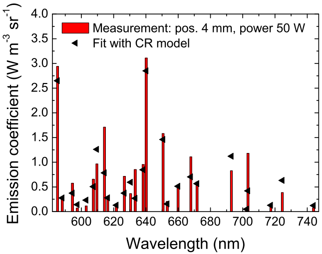

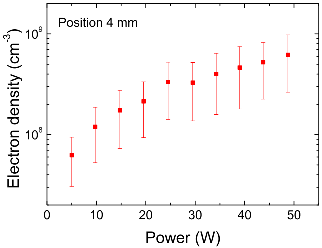

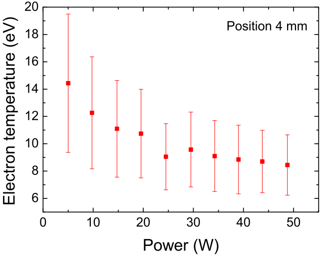

Navrátil Z, Dvořák P, Brzobohatý O and Trunec D 2010 *J. Phys. D: Appl. Phys.* 43(50) 505203.

MW surface-wave driven discharge in neon in coaxial configuration

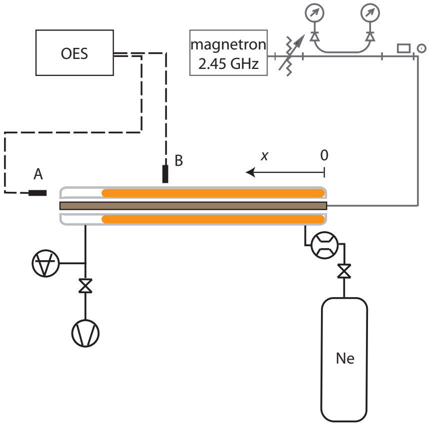

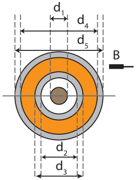


argon

- two-cylinder quartz tube with copper rod antenna, length 320 mm, dimensions $d_1 = 5$ mm, $d_2 = 7$ mm, $d_3 = 11$ mm, $d_4 = 20$ mm and $d_5 = 24$ mm
- microwave power 60 W
- pressure 300 – 700 Pa of neon with research purity 99.999%, flow rate 6 – 30 sccm

Electron distribution function

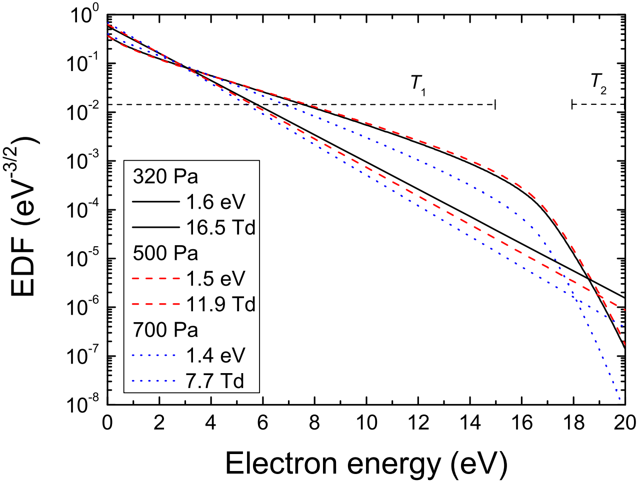

$$T_1 = 2.1 - 2.5 \text{ eV}, \qquad \mathscr{E} < 15\,\text{eV}$$

$$T_2 = 0.33 - 0.43 \text{ eV}, \quad 18\,\text{eV} < \mathscr{E} < 20\,\text{eV}$$

Spectra fit

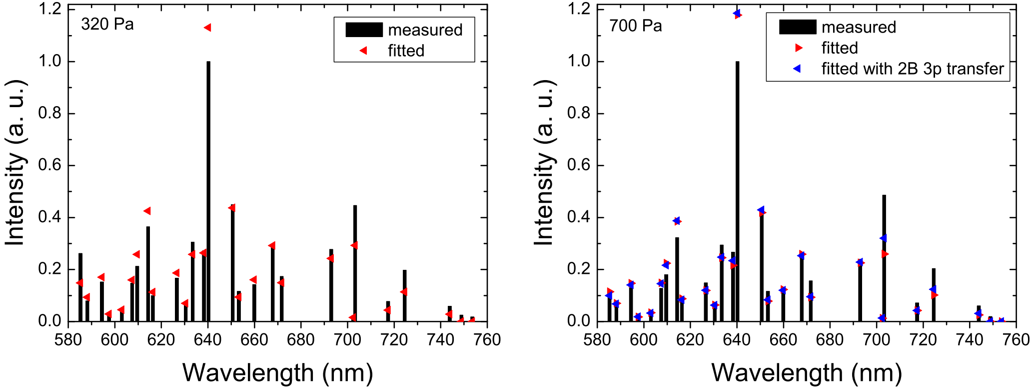

- using BKE solver
- effect of deactivation by heavy particles on spectra under studied conditions is small

Sensitivity to electron density and metastable density

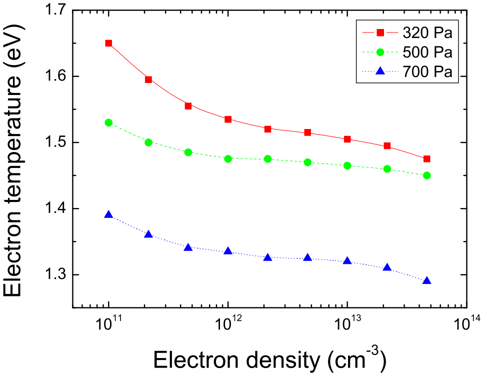

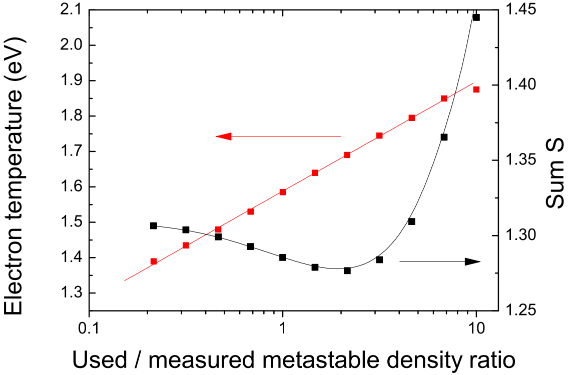

sensitivity to metastables: 0.3 eV or 2 Td per order of density

Axial dependencies for $T = 300$ K

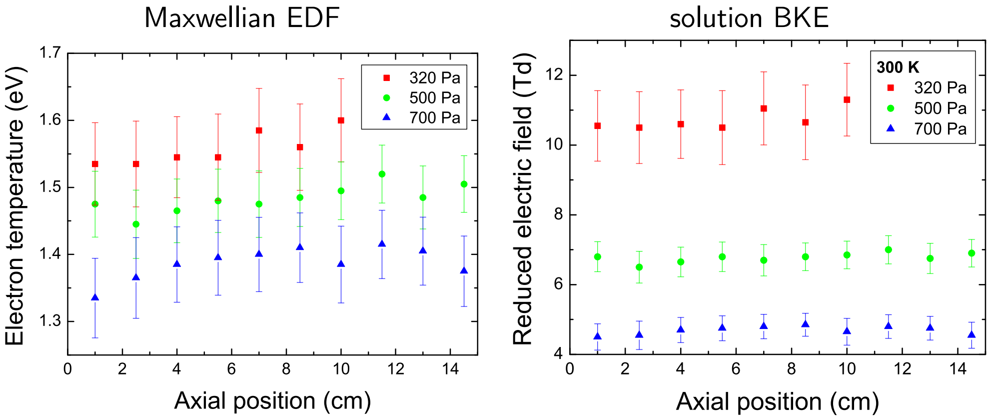

N_2 rotational temperature in $C\,^3\Pi_u$ state

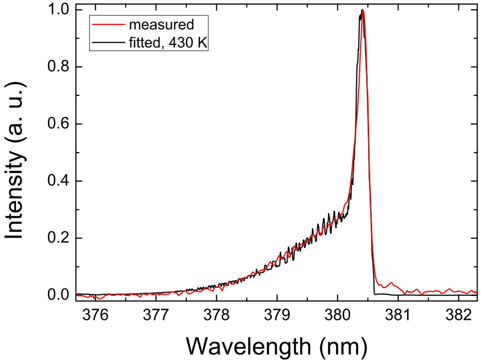

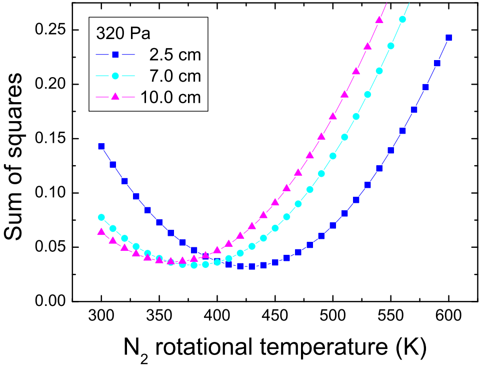

Program Specair. Laux C O 2002. In Fletcher D, Charbonnier J M, Sarma G S R and Magin T, eds., *von Karman Institute Lecture Series 2002–07, Physico-Chemical Modeling of High Enthalpy and Plasma Flows* Rhode-Saint-Gencse, Belgium.

N_2 rotational temperature in $C\,^3\Pi_u$ state

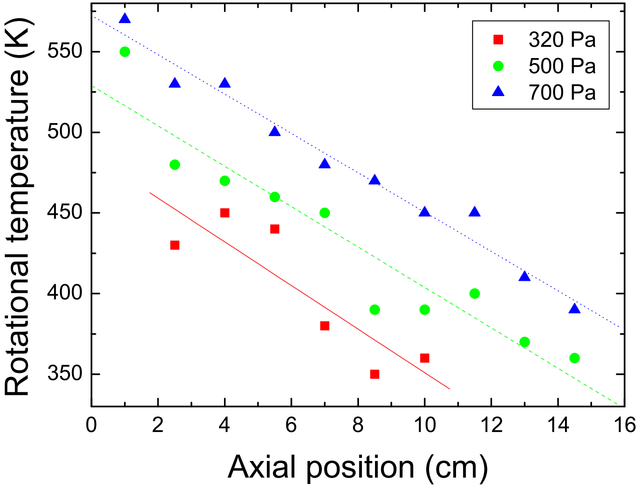

Effect of gas temperature

300 K

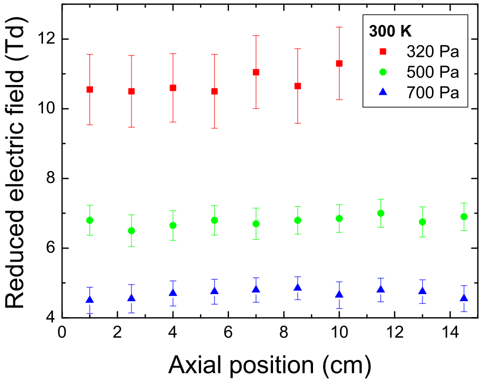

N_2 rotational temperature

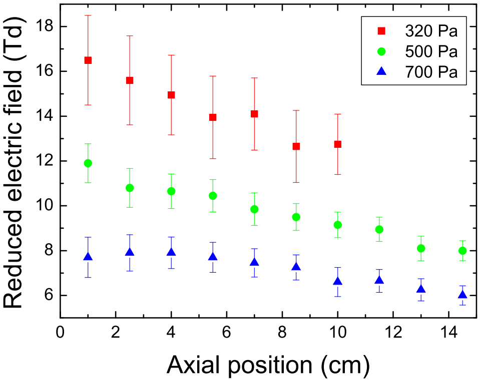

- heating by oscillating field is governed by E/N and ω/N, elastic collisions inhance heating
- ω/N is not constant along the column

Self-absorption

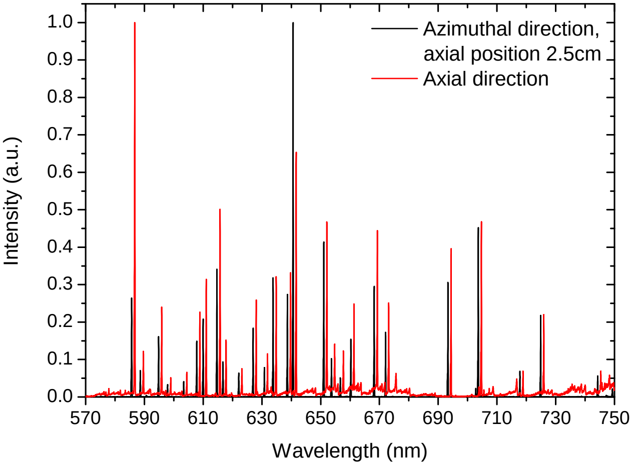

Effective branching fractions Γ_{ij}

- isolated atom

$$\Gamma_{ij} = \frac{A_{ij}}{\sum_l A_{il}}$$

- plasma

$$\Gamma_{ij}^{\mathrm{eff}} = \frac{g(k_{ij}^0 L) A_{ij}}{\sum_l g(k_{il}^0 L) A_{il}}$$

- absorption coefficient

$$k_{ij}^0 = \frac{\lambda_{ij}^3}{8\pi^{3/2}} \sqrt{\frac{m_0}{2k_\mathrm{b} T}} \frac{g_i}{g_j} A_{ij} n_j$$

- measured

$$\Gamma_{ij}^{\mathrm{exp}} = \frac{I_{ij}/h\nu_{ij}}{\sum_l I_{il}/h\nu_{il}}$$

Escape factor

- Mewe approximate expression

$$g(k_{ij}^0 L) = \frac{2 - e^{-k_{ij}^0 L/1000}}{1 + k_{ij}^0 L}$$

- assumption of homogeneous distribution of atoms
- e.g. Ar $2p_6 \rightarrow 1s_5$ (763.5 nm), $\rho = 10\,\mathrm{cm}$

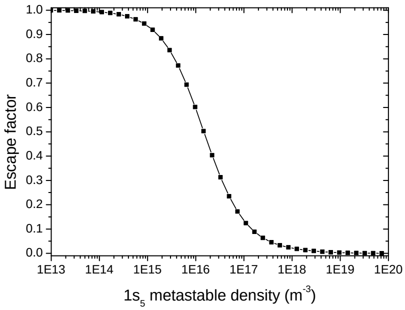

Example – density of Ti and Ti^+ in magnetron discharge

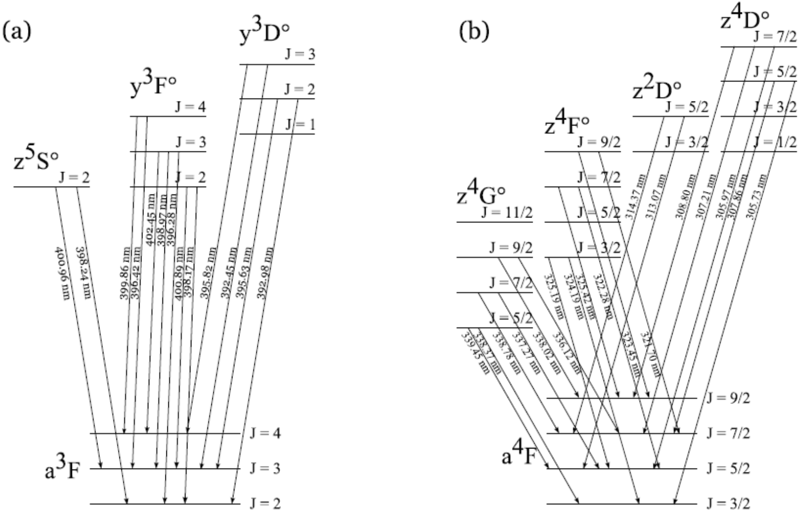

Figure 1. Energy levels and selected transitions for density measurement of (a) Ti neutral atom and (b) Ti ion.

Example – density of Ti and Ti^+ in magnetron discharge

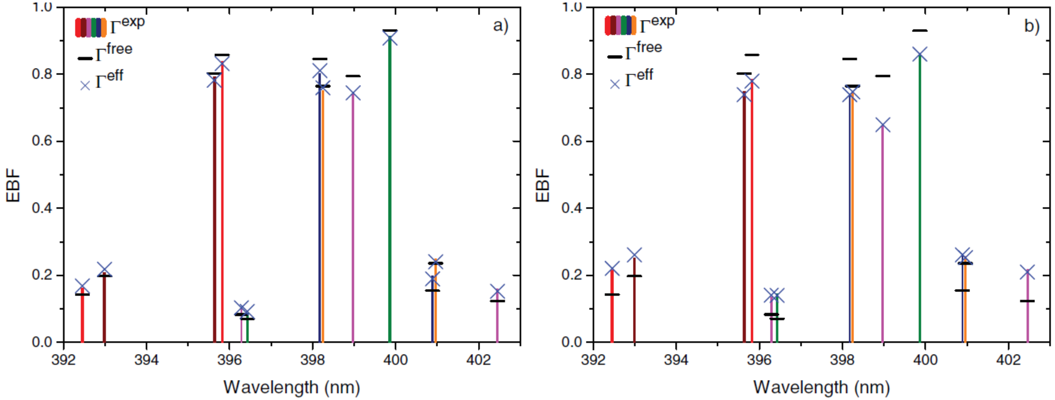

Example – density of Ti and Ti^+ in magnetron discharge